
**Liquid Crystals**
Publication details, including instructions for authors and subscription information:
http://www.informaworld.com/smpp/title~content=t713926090

# Stationary states of hybrid aligned flexoelectric nematic layers

Grzegorz Derfel[a]
[a] Institute of Physics, Technical University of Łódź, 90-924 Łódź, Poland

**To cite this Article** Derfel, Grzegorz(2007) 'Stationary states of hybrid aligned flexoelectric nematic layers', Liquid Crystals, 34: 10, 1201 — 1214
**To link to this Article: DOI:** 10.1080/02678290701640256
**URL:** http://dx.doi.org/10.1080/02678290701640256

*Liquid Crystals*, Vol. 34, No. 10, October 2007, 1201–1214



# Stationary states of hybrid aligned flexoelectric nematic layers

GRZEGORZ DERFEL*
Institute of Physics, Technical University of Łódź, ul. Wólczańska 219, 90-924 Łódź, Poland

(*Received 23 April 2007; in final form 13 August 2007; accepted 14 August 2007*)

Nematic layers, with planar anchoring conditions on one boundary plate and homeotropic anchoring conditions on the other, subjected to an external electric field may adopt planar, distorted or homeotropic structure depending on the anchoring strength and dielectric anisotropy. The influence of flexoelectric properties on stability of the planar and homeotropic structures with respect to small distortions is studied. The case of a positive sum of the flexoelectric coefficients $e>0$ is considered under the assumption that the anchoring strength on the planar wall, $W_1$, is greater than that on the homeotropic boundary, $W_2$. In the presence of flexoelectricity, one sign of the bias voltage $U$ is distinguished. In the case considered, the planar and homeotropic structures are favoured if the higher electric potential is applied to the homeotropically aligning electrode. If the applied voltage has the reverse sign, the distorted structure prevails. In a flexoelectric nematic possessing positive dielectric anisotropy, $\Delta\varepsilon>0$, the planar structure may exist in thicker layers and in a wider range of voltages than in the non-flexoelectric nematic. The homeotropic state is favoured by weak flexoelectricity, i.e. the range of thickness in which this state is stable at given voltage is wider than in the non-flexoelectric case. For moderate values of $e$, the homeotropic state appears for a range of thickness that increases with $U$ but narrows with increasing $e$. When the flexoelectric properties are too strong, i.e. when $e$ exceeds a critical value dependent on $W_1/W_2$, the homeotropic structure is excluded. If $\Delta\varepsilon\leqslant 0$, the planar structure is realized if the thickness belongs to some range the width of which increases with $U$. The homeotropic state does not occur. These results, obtained for the insulating nematics, are valid quantitatively also for the case of conducting nematics only if the ion concentration is smaller than ca. $5\times10^{18}\,\mathrm{m}^{-3}$. A method of measurement of $e$ based on the above results is proposed. The examples of representative transitions between the planar, distorted and homeotropic structures obtained numerically are presented. Possible advantages of hybrid aligned flexoelectric nematic layers for display applications are discussed.



## 1. Introduction

Liquid crystal layers confined between transparent electrodes are basic components of liquid crystal devices of any type. They serve also as samples commonly used in fundamental research on liquid crystals. The hybrid aligned nematic (HAN) layer belongs to the most often investigated liquid crystalline systems. In this geometry, the inner surfaces of the cell are suitably prepared in order to obtain specific directions of the easy axes, i.e. of the preferred orientations adopted by the director **n** when it is aligned only by the interaction with the substrate. On one surface, the planar alignment is imposed (i.e. the easy axis $\mathbf{e_1}$ is parallel to the substrate) whereas on the other surface the easy axis $\mathbf{e_2}$ has the homeotropic orientation (i.e. perpendicular to the substrate). If the layer is not subjected to any external interaction, the director undergoes a smooth tilt from one surface to the other. Its orientation on the surfaces may deviate from the strictly planar or strictly homeotropic if the anchoring energies are small. Such director distribution contains splay and bend deformations. External electric or magnetic fields influence the director distribution and change the optical properties of the layer. The electro-optical effect in the HAN layer was proposed for display applications 30 years ago [1]. It offers fast thresholdless response to the bias voltage.

Calculations based on the elastic continuum theory [2, 3] show that when the planar and homeotropic anchoring strengths, (denoted here by $W_1$ and $W_2$, respectively) are not equal, there is a critical layer thickness, $d_c$, below which the director field throughout the layer adopts the uniform orientation imposed by the stronger anchoring. If the layer is sufficiently thick or if $W_1=W_2$, the distorted director distribution described above occurs.

The main contribution deciding on the behaviour of the HAN layer in the external electric field is the bulk

* Email: gderfel@p.lodz.pl

*Liquid Crystals*
ISSN 0267-8292 print/ISSN 1366-5855 online © 2007 Taylor & Francis
http://www.tandf.co.uk/journals
DOI: 10.1080/02678290701640256

torque due to the dielectric anisotropy, $\Delta\varepsilon$. Deformation of dielectric nature is a quadratic effect and therefore does not depend on the sign of the voltage. However the nematic materials usually possess flexoelectric properties due to asymmetric shape and dipolar nature of mesogenic molecules [4]. Flexoelectricity manifests itself by an electric polarization whenever the director distribution contains splay or bend (which is called the direct flexoelectric effect), as well as by deformation resulting from the interaction between the flexoelectric polarization and the applied electric field (which is known as the converse flexoelectric effect). In both cases, the coupling of the field with the flexoelectric polarization is linear. The field effects depend therefore on the sign of the bias voltage. The flexoelectric properties are described by two flexoelectric coefficients, $e_{11}$ and $e_{33}$, which determine the relationship between the deformation of the nematic and the electric polarization $\mathbf{P}=e_{11}\mathbf{n}(\nabla\cdot\mathbf{n})-e_{33}\mathbf{n}\times(\nabla\times\mathbf{n})$. Their values are of the order of $\mathrm{pC\,m^{-1}}$ and are difficult to measure (for a review, see Petrov [5]). The role of flexoelectricity in the behaviour of liquid crystal systems has been investigated by many authors. Flexoelectric properties are evident in experiments performed with HAN layers [6, 7] and should be taken into account in interpretation of the experimental results [8, 9]. They also play a crucial role in the zenithal bistable device (ZBD) displays in which the hybrid structure arises as one of the stable states [10, 11]. The HAN layers are also often used in experiments carried out to determine the flexoelectric coefficients [7, 12, 13].

The behaviour of the non-flexoelectric hybrid aligned layer under the action of an external electric field was described theoretically by Barbero and co-workers [2, 3] for the case of a negative dielectric anisotropy and prevailing homeotropic anchoring strength, $W_2\geqslant W_1$. They determined the ranges of thickness and of the electric field strengths in which the planar and homeotropic states are stable. They found that in the absence of the field the homeotropic structure is stable if the layer is thinner than $d_c=L_2-L_1$, where $L_1=k_{33}/W_1$ and $L_2=k_{33}/W_2$ are the extrapolation lengths and $k_{33}$ is the bending elastic constant. Above $d_c$ the distorted structure occurs. The homeotropic state existing in the thin layer is destroyed if the critical field is exceeded. Sufficiently high electric field induces the planar structure. If $W_1=W_2=W$, the homeotropic state cannot exist and the planar state arises above the electric field strength given by $E=(W/k_{33})[k_{33}/(\varepsilon_0|\Delta\varepsilon|)]^{1/2}$, where $\varepsilon_0$ is the permittivity of free space. Analogous results can be expected in the case of $\Delta\varepsilon>0$ and $W_2\leqslant W_1$. The planar structure is replaced by the homeotropic alignment and vice versa. The corresponding formulae can be obtained if $k_{33}$ is replaced by the splay elastic constant $k_{11}$.

In this paper, the hybrid aligned flexoelectric nematic (HAFN) layer subjected to an electric field is studied theoretically. The role of the flexoelectricity in the stability of the planar and homeotropic structures is determined. Prevailing planar anchoring strength, $W_1\geqslant W_2$, was assumed. Both signs of the dielectric anisotropy as well as the case of a dielectrically compensated nematic, $\Delta\varepsilon=0$, were considered. Since the director is restricted to a plane perpendicular to the layer and the electric field is also normal to the layer, only the sum of the flexoelectric coefficients $e=e_{11}+e_{33}$ is essential [14]. A positive sign for $e$ was assumed. The thickness, $d$, and voltage, $U$, were chosen as control parameters. The ranges of stability of the planar and homeotropic states in the $U,d$-plane are determined.

The main results can be briefly summarized as follows. In a layer of a flexoelectric nematic possessing positive dielectric anisotropy, $\Delta\varepsilon>0$, flexoelectricity favours the occurrence of planar structure in some range of positive voltages. The planar states may be induced in much thicker layers than in the case of a non-flexoelectric nematic. On the other hand, flexoelectricity narrows the range of voltages in which the homeotropic state is stable. If the flexoelectric properties are too strong, the homeotropic state becomes unstable. In a nematic layer characterized by $\Delta\varepsilon\leqslant 0$, the homeotropic state does not occur. The influence of flexoelectric properties manifests itself by a shift of the voltage range, in which the planar structure exists, towards the lower values.

Additional numerical simulations of the HAFN layers were performed for nematics containing ions. These showed that the theoretical results obtained for insulating nematics can be applied to the case of real conducting nematics only if the ion concentration is of the order $5\times10^{18}\,\mathrm{m^{-3}}$ or lower. This statement allows an alternative method of measurement of the flexoelectric coefficients to be proposed.

The paper is organized as follows. In section 2, the assumptions and geometry of the system under consideration are described. In section 3, the case of $\Delta\varepsilon>0$ is considered. In section 3.1, the applied approach is described and the stability of the planar state is analysed. Section 3.2 concerns the stability of the homeotropic structure. Sections 4 and 5 are devoted to the stability of the planar structure in the cases of $\Delta\varepsilon<0$ and $\Delta\varepsilon=0$, respectively. Section 6 presents examples of the transitions between planar, distorted and homeotropic states found by means of numerical simulations. Section 7 is devoted to discussion of the results.

## 2. Assumptions and geometry of the system

A hybrid aligned flexoelectric nematic layer of thickness $d$ is considered. The nematic liquid crystal is confined between two infinite plates, which play the role of electrodes and are parallel to the $x$,$y$-plane of the Cartesian coordinate system and positioned at $z=0$ and $z=d$. A voltage $U$ is applied between them; the lower electrode ($z=0$) was earthed. The director $\hat{n}$ is parallel to the $y$,$z$-plane. Hybrid boundary conditions were assumed with planar orientation of the easy axis $\mathbf{e_1}(0,1,0)$ at $z=0$ and homeotropic orientation of $\mathbf{e_2}(0,0,1)$ at $z=d$. The planar anchoring strength $W_1$ was assumed to be greater than the homeotropic anchoring strength $W_2$ or equal to $W_2$. The model substance was characterized by the positive sum of the flexoelectric coefficients, $e=e_{11}+e_{33}$. Both signs of dielectric anisotropy, $\Delta\varepsilon$, as well as the case of $\Delta\varepsilon=0$ were taken into account. Fixed elastic constants, $k_{11}=6.2\,\mathrm{pN}$ and $k_{33}=8.6\,\mathrm{pN}$, were used in all the numerical examples given in the following. The theoretical analysis was performed ignoring the presence of ions in the nematic material. The role of the ionic charge is discussed on the basis of preliminary numerical calculations.

## 3. Positive dielectric anisotropy

In the case of a positive dielectric anisotropy, the dielectric torque may lead to the homeotropic structure. The planar structure is stable in the absence of the field and its occurrence in the presence of weak fields is also plausible. Therefore stability of each of these states should be analysed.

### 3.1. *Stability of the planar structure in the case of a positive dielectric anisotropy*

In this section, the director orientation is described by means of the angle $\theta$ measured between the director and the $y$ axis. The volume free energy density is given by the formula

$$g_v=\frac{1}{2}\left(k_{33}\sin^2\theta+k_{11}\cos^2\theta\right)\left(\frac{\mathrm{d}\theta}{\mathrm{d}z}\right)^2 -\frac{1}{2}\varepsilon_0\left(\varepsilon_\perp+\Delta\varepsilon\sin^2\theta\right)\left(\frac{\mathrm{d}V}{\mathrm{d}z}\right)^2+\frac{e}{2}\sin 2\theta\frac{\mathrm{d}\theta}{\mathrm{d}z}\frac{\mathrm{d}V}{\mathrm{d}z}, \quad (1)$$

where $V$ is the electric potential. The anchoring energy on the planar wall is assumed to be in the form

$$g_{s1}=-\frac{1}{2}W_1\cos^2\theta(0) \quad (2)$$

and on the homeotropic wall in the form

$$g_{s2}=-\frac{1}{2}W_2\sin^2\theta(d). \quad (3)$$

The torque equation for the bulk reads

$$\begin{aligned}&\frac{1}{2}(k_{33}-k_{11})\sin 2\theta\left(\frac{\mathrm{d}\theta}{\mathrm{d}z}\right)^2\\&+\left(k_{33}\sin^2\theta+k_{11}\cos^2\theta\right)\frac{\mathrm{d}^2\theta}{\mathrm{d}z^2}\\&+\frac{1}{2}\varepsilon_0\Delta\varepsilon\sin 2\theta\left(\frac{\mathrm{d}V}{\mathrm{d}z}\right)^2\\&+\frac{e}{2}\sin 2\theta\left(\frac{\mathrm{d}^2V}{\mathrm{d}z^2}\right)=0.\end{aligned} \quad (4)$$

The boundary conditions for $\theta$ are expressed by the surface torque equations

$$-\frac{e}{2}\sin(2\theta(0))\frac{\mathrm{d}V}{\mathrm{d}z}\bigg|_0-\left(k_{33}\sin^2\theta(0)+k_{11}\cos^2\theta(0)\right)\frac{\mathrm{d}\theta}{\mathrm{d}z}\bigg|_0+\frac{1}{2}W_1\sin(2\theta(0))=0 \quad (5)$$

$$\frac{e}{2}\sin(2\theta(d))\frac{\mathrm{d}V}{\mathrm{d}z}\bigg|_d+\left(k_{33}\sin^2\theta(d)+k_{11}\cos^2\theta(d)\right)\frac{\mathrm{d}\theta}{\mathrm{d}z}\bigg|_d-\frac{1}{2}W_2\sin(2\theta(d))=0. \quad (6)$$

The structure of the layer is also determined by the electrostatic equation

$$\varepsilon_0\left(\varepsilon_\perp+\Delta\varepsilon\sin^2\theta\right)\frac{\mathrm{d}^2V}{\mathrm{d}z^2}+\varepsilon_0\Delta\varepsilon\sin 2\theta\frac{\mathrm{d}V}{\mathrm{d}z}\frac{\mathrm{d}\theta}{\mathrm{d}z} -e\cos 2\theta\left(\frac{\mathrm{d}\theta}{\mathrm{d}z}\right)^2-\frac{e}{2}\sin 2\theta\frac{\mathrm{d}^2\theta}{\mathrm{d}z^2}=0, \quad (7)$$

with the boundary conditions for the electric potential $V(0)=0$ and $V(d)=U$.

In order to study the stability of the planar state in the HAFN layer, small distortions described by $\theta\ll 1$ should be considered. With this approximation, the bulk torque equation (4) takes the linearized form

$$\frac{\mathrm{d}^2\theta}{\mathrm{d}z^2}+\kappa^2\theta=0, \quad (8)$$

where $\kappa=(U/d)(\varepsilon_0\Delta\varepsilon/k_{11})^{1/2}$. The electrostatic equation (7) reduces to $\mathrm{d}^2V/\mathrm{d}z^2=0$, which is also used in derivation of equation (8). The solution of equation (8) has the form

$$\theta(z)=A\cos(\kappa z)+B\sin(\kappa z), \quad (9)$$

where $A$ and $B$ are the integration constants. The planar

state is determined by $A=0$ and $B=0$. Its stability with respect to small deformations described by the solution of equation (9) will be studied. For this purpose, the free energy per unit area of the layer is expressed as a function of $A$ and $B$. According to the assumption $\theta \ll 1$, only the quadratic terms in $A$ and $B$ are retained. In this approximation, the volume free energy density has the form

$$\begin{aligned} g_v = & \frac{1}{2} k_{11} \kappa^2 \\ & \left[ \left(B^2 - A^2\right) (\cos(2\kappa z) + f \sin(2\kappa z)) \right. \\ & \left. + AB(f \cos(2\kappa z) - \sin(2\kappa z)) \right], \end{aligned} \tag{10}$$

where $f = e(k_{11}\varepsilon_0 \Delta\varepsilon)^{-1/2}$. The surface anchoring energies are $g_{s1} = -\frac{1}{2} W_1 \left(1 - A^2\right)$ at $z=0$, and $g_{s2} = -\frac{1}{2} W_2 \left(A^2 \cos^2 \kappa d + AB \sin 2\kappa d + B^2 \sin^2 \kappa d\right)$ at $z=d$. The total free energy per unit area of the layer is given by

$$\begin{aligned} G = & \frac{1}{2} A^2 k_{11} \left(-\kappa sc - f\kappa s^2 + 1/L_1 - c^2/L_2\right) \\ & + ABk_{11} \left(-\kappa s^2 + f\kappa sc - sc/L_2\right) \\ & + \frac{1}{2} B^2 k_{11} \left(\kappa sc + f\kappa s^2 - s^2/L_2\right), \end{aligned} \tag{11}$$

where $L_i = k_{11}/W_i > 0$ are the extrapolation lengths and the abbreviations $\sin \kappa d = s$ and $\cos \kappa d = c$ are introduced. In practice, the electric field arises due to the external voltage, $U$, applied between the electrodes, which are also the walls of the layer. This means that the bias voltage plays the role of a control parameter. Therefore, it is useful to determine the range of existence of the planar state in the $U,d$-plane. For this reason, in the following, $\kappa$ is replaced by $u/d$, which gives $s = \sin u$ and $c = \cos u$, where $u = U(\varepsilon_0 \Delta\varepsilon / k_{11})^{1/2}$ is the dimensionless voltage.

The planar state is stable if the function $G$ has a minimum for $A=0$ and $B=0$. The stability condition is expressed by two inequalities

$$\left(\partial^2 G/\partial A^2\right)\left(\partial^2 G/\partial B^2\right) - \left(\partial^2 G/\partial A \partial B\right)^2 > 0 \tag{12}$$

and

$$\partial^2 G/\partial B^2 > 0. \tag{13}$$

Solutions of these inequalities should satisfy the additional obvious condition

$$d > 0. \tag{14}$$

Condition (12) reads

$$\begin{aligned} -d^2 + \mathrm{d}u[f(L_2 + L_1) + (L_2 - L_1)\cot u] \\ - u^2 \left(1 + f^2\right) L_1 L_2 > 0. \end{aligned} \tag{15}$$

This quadratic inequality gives a relationship between the thickness of the layer and the bias voltage included in the parameter $u$. For given $U$, equation (15) is satisfied if

$$d_1^+ < d < d_1^-, \tag{16}$$

where

$$d_1^{\pm} = \left(-\beta \pm \Delta^{1/2}\right) \Big/ (2\alpha) \tag{17}$$

with $\alpha = -1$, $\beta = u[f(L_2 + L_1) + (L_2 - L_1)\cot u]$, $\gamma = -u^2(1 + f^2) L_1 L_2$ and $\Delta = \beta^2 - 4\alpha\gamma$.

Condition (13) takes the form

$$-d + uL_2(\cot u + f) > 0, \tag{18}$$

which is equivalent to equation (15) if $L_1 = 0$. Its solution is determined by

$$d < uL_2(\cot u + f) \equiv d_2. \tag{19}$$

Comparison of equations (17) and (19) shows that $d_2 > d_1^-$ (see appendix). This means that whenever inequality (12) is true, condition (13) is also satisfied. The superposition of equations (18) and (15) is identical with equation (15), which therefore yields the condition sufficient for stability of the planar state. Equation (17) gives two branches of the curve surrounding the region in the $U,d$-plane in which the planar state exists.

In general, an explicit form of equation (17) is not very useful because of its complexity. The same concerns the condition $\Delta = 0$, which in principle allows determination of the range of $U$ in which solutions to equation (16) exist. Simple analytical expressions can be obtained only in several particular cases:

(i) $L_1 = L_2$: if the anchoring strengths on the planar and homeotropic walls are identical, then $\Delta < 0$. This means that inequality (12) has no solution, i.e. the planar state does not exist.

(ii) $L_1 = 0$: the results obtained for the case of a rigid planar anchoring are identical with equations (19) and (14): $d_1^- = uL_2(\cot u + f)$ and $d_1^+ = 0$. They determine the upper and the lower boundaries of the region of existence of the planar state in the $U,d$-plane. At $U=0$, the upper branch reaches $d_1^-(0) = L_2$. It ends when $d_1^- = 0$, i.e. for positive $u_1 = \cot^{-1}(-f)$ and for negative $u_2 = u_1 - \pi$.

(iii) $U=0$: in the absence of an external voltage, the planar state exists in the layers of thickness $d < L_2 - L_1$. This result can be obtained from equation (15), which in the limit $u \to 0$ gives $-d^2 + d(L_2 - L_1) u \cot u > 0$ and leads to $0 < d < L_2 - L_1$ since $\lim_{u \to 0} u \cot u = 1$. This result is

in agreement with the analogous case obtained Barbero and Barberi [2] for non-flexoelectric nematics.

Figure 1 shows several representative results for various sums of the flexoelectric coefficients and three ratios between planar and homeotropic anchoring strengths. In the case of a non-flexoelectric nematic, the planar state appears for $d$ and $U$ from a closed region in the $U$,$d$-plane. This region has a regular shape, symmetric with respect to $U=0$. The flexoelectricity introduces an asymmetry since its linear coupling with the electric field makes the voltages of opposite signs non-equivalent. In the present case of $e>0$, the flexoelectricity enhances the region of existence of the planar state induced by the positive voltage and diminishes the region corresponding to the negative voltage. This effect is the more pronounced the higher is the value of parameter $f$, i.e. the stronger are the flexoelectric properties or the smaller is the dielectric anisotropy. When $\Delta\varepsilon\rightarrow 0$, the range of positive voltage favouring the planar state tends to infinity. Figure 2 shows examples of the regions of existence of the planar state for four values of $\Delta\varepsilon$. These regions are always restricted to closed areas spreading over the large positive voltages when $\Delta\varepsilon\rightarrow 0$.

In the above examples, the value of $L_2$ is maintained constant. If the planar anchoring strength increases, i.e. if $L_1$ becomes smaller, the planar structure occurs in a larger region. (Additional calculations show that if $W_2$ is enhanced, the planar structure is restricted to thinner layers.) If the planar anchoring is rigid, the ranges of $U$ and $d$ are the largest.

### 3.2. *Stability of the homeotropic structure in the case of a positive dielectric anisotropy*

In analogy to the results reported by Barbero and Barberi [2], one may suppose that if the electric field strength parameter $\kappa$ is sufficiently large, the homeotropic structure becomes stable and replaces the distorted state. The coherence length, $1/\kappa$, corresponding to this critical field is equal to $(L_1L_2)^{-1/2}$. Of course, if the planar anchoring is rigid, the homeotropic state cannot appear.

In this section, the influence of flexoelectricity on this effect is studied. The stability of the homeotropic state induced by the electric field is investigated by means of the same approach as in the preceding section. In order to obtain the truncated free energy function, the angle $\vartheta=90^\circ-\theta$ is introduced. It is measured between the director and the $z$ axis. Small distortions of the homeotropic structure are characterized by $\vartheta\ll 1$.

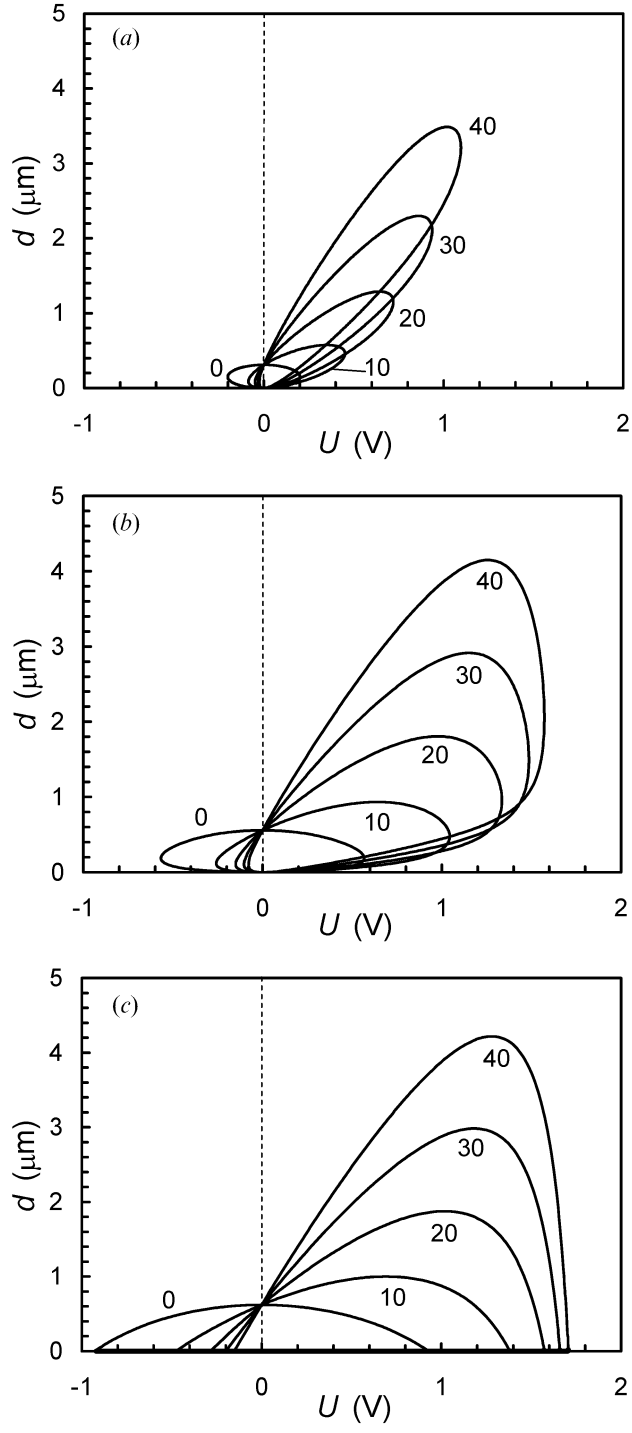


Figure 1. Regions of stability of the planar state for $\Delta\varepsilon=2$ and $W_2=10^{-5}\,\mathrm{J\,m^{-2}}$. (a) $W_1=2\times10^{-5}\,\mathrm{J\,m^{-2}}$, (b) $W_1=10^{-4}\,\mathrm{J\,m^{-2}}$, (c) $W_1=\infty$. The values of $e$ (in $\mathrm{pC\,m^{-1}}$) are indicated for each curve.

The linearized torque equation for the bulk has now the form

$$\frac{\mathrm{d}^2\vartheta}{\mathrm{d}z^2}-\lambda^2\vartheta=0, \tag{20}$$

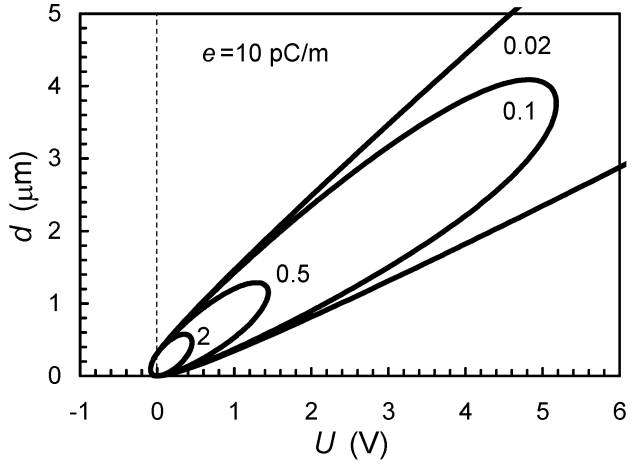


Figure 2. Regions of stability of the planar state for $W_2=10^{-5}\,\mathrm{J\,m^{-2}}$ and $e=10\,\mathrm{pC\,m^{-1}}$ calculated for several values of $\Delta\varepsilon$ indicated for each curve.

where $\lambda=v/d$, $v=U(\varepsilon_0\Delta\varepsilon/k_{33})^{1/2}=u/\sqrt{b}$ and $b=k_{33}/k_{11}$. The solution of this equation is $\vartheta(z)=C\cosh(\lambda z)+D\sinh(\lambda z)$, where $C$ and $D$ are constants. The total free energy per unit area of the layer is given by

$$G=\frac{1}{2}C^2k_{33}\left[\lambda sc-g\lambda s^2-1/(bL_1)+c^2/(bL_2)\right]+CDk_{33}\left[\lambda s^2-g\lambda sc+sc/(bL_2)\right]+\frac{1}{2}D^2k_{33}\left[\lambda sc-g\lambda s^2+s^2/(bL_2)\right], \tag{21}$$

where $g=e(k_{33}\varepsilon_0\Delta\varepsilon)^{-1/2}=f/\sqrt{b}$, $s=\sinh\lambda d=\sinh v$, $c=\cosh\lambda d=\cosh v$ and $L_i>0$. This function possesses a minimum at $C=0$ and $D=0$ (which denotes the homeotropic state) if the two inequalities are satisfied:

$$-d^2+dvb[g(L_2+L_1)-(L_2-L_1)\coth v]+v^2b^2(1-g^2)L_1L_2>0 \tag{22}$$

and

$$vbL_2(g-\coth v)-d<0. \tag{23}$$

**3.2.1. Analysis of condition (22).** Inequality (22) has two solutions of the same form as equation (17). The solution for $U>0$ is

$$\min\left(d_3^+,\,d_3^-\right)<d<\max\left(d_3^+,\,d_3^-\right), \tag{24}$$

and that for $U<0$ reads

$$\min\left(d_4^+,\,d_4^-\right)<d<\max\left(d_4^+,\,d_4^-\right), \tag{25}$$

The limiting thicknesses in equations (24)–(25) are given by

$$d_i^{\pm}=\left(-\beta\pm\Delta^{1/2}\right)\Big/(2\alpha) \tag{26}$$

with $\alpha=-1$, $\beta=vb[g(L_2+L_1)-(L_2-L_1)\coth v]$, $\gamma=v^2b^2(1-g^2)L_1L_2$ and $\Delta=\beta^2-4\alpha\gamma$. In the general case, the analysis of these formulae is difficult. Nevertheless, the numerical results (which are exemplified in the following) suggest that $\Delta>0$ for sufficiently high $|U|$. In the limit $v\to+\infty$, when $\coth v=1$, the critical thicknesses $d_3^{\pm}$ are

$$d_{3\infty}^-=vbL_1(g+1) \tag{27}$$

and

$$d_{3\infty}^+=vbL_2(g-1). \tag{28}$$

In the limit $v\to-\infty$, when $\coth v=-1$, the critical thicknesses $d_4^{\pm}$ are

$$d_{4\infty}^+=vbL_1(g-1) \tag{29}$$

and

$$d_{4\infty}^-=vbL_2(g+1). \tag{30}$$

These formulae give the equations of oblique asymptotes $d(U)$. The solutions of equation (22) determine the ranges (24) and (25) that are included between halves of these asymptotes corresponding to $U>0$ and $U<0$, respectively. For given $L_2$ and $L_1$, the relationships between $d_{3\infty}^+$, $d_{3\infty}^-$, $d_{4\infty}^+$ and $d_{4\infty}^-$ depend on the flexoelectric properties as well as on the dielectric anisotropy involved in $g$.

(1) For weak flexoelectric properties, $0\leqslant g\leqslant 1$, for positive voltage, the function $d_{3\infty}^+(U)$ given by equation (28) takes negative values. In consequence, condition (22) is satisfied if the thickness determined by equation (24) belongs to the range

$$(0,\,vbL_1(g+1)), \tag{31}$$

which results from equations (27) and (14). For $U<0$, the values of $d_{4\infty}^+(U)$ given by equation (30) are negative. Therefore the corresponding range including the solution (25) is determined by equations (14) and (29):

$$(0,\,vbL_1(g-1)). \tag{32}$$

(2) For moderate flexoelectric properties, $1<g\leqslant(L_2+L_1)/(L_2-L_1)$, the asymptotes that determine the positive values of thickness occur only for $U>0$. The solutions of equation (22) are described by equation (24) and included within the range

$$(vbL_2(g-1),\ vbL_1(g+1)). \tag{33}$$

If $g=(L_2+L_1)/(L_2-L_1)$, the range (33) shrinks to a point and its limits given by equations (27)–(28) interchange.

(3) For strong flexoelectric properties, $g>(L_2+L_1)/(L_2-L_1)$, the range of thickness given by equation (24) is included in

$$(vbL_1(g+1),\ vbL_2(g-1)). \tag{34}$$

**3.2.2. Analysis of condition (23).** The second condition, expressed by the inequality (23), has the solution

$$d>vbL_2(g-\coth v)\equiv d_5. \tag{35}$$

Two ranges of $g$ can be distinguished.

(1) For moderate and strong flexoelectric properties, $g>1$, for positive voltages, condition (23) is satisfied if $v>\coth^{-1}g$. For $U\to\infty$, the thickness $d_5(U)$ tends to the asymptote $d=vbL_2(g-1)$, identical with equation (28). For $U\to-\infty$, the asymptote is $d=vbL_2(g+1)$ [identical with equation (30)] and takes negative values. Therefore, condition (23) is certainly true for the thickness that belongs to the range

$$(vbL_2(g-1),\ \infty), \tag{36}$$

when $U>0$, and to the range

$$(0,\ \infty), \tag{37}$$

when $U<0$ (since $d>0$).

(2) For weak flexoelectric properties, $0\leqslant g\leqslant 1$, both asymptotes predict negative $d_5$. In consequence, condition (23) is satisfied in the range $(0, \infty)$ at any voltage.

**3.2.3. Superposition of conditions (22) and (23).** In order to determine the range of stability of the homeotropic state one must find superposition of conditions (22)–(23), i.e. the superposition of their solutions expressed by equations (24) and (35) or by equations (25) and (35). The results can be recognized by comparison of the slopes of asymptotes. They are illustrated in the $U,d$-plane in figures 3 a and 3 b. The boundaries of the regions of existence of the homeotropic state tend to the asymptotes when $U\to\infty$ or $d\to\infty$. When $L_1=L_2$, these boundaries coincide with the asymptotes.

The above results can be systematized as follows:

(1) For a non-flexoelectric nematic, $g=0$, the homeotropic state appears if the thickness is smaller than a critical value. Since this value is independent of the sign of the voltage, the regions of stability of the homeotropic state in the $U,d$-plane are symmetrical with respect to $U=0$.

(2) For weak flexoelectric properties, $0<g\leqslant 1$, flexoelectricity introduces an asymmetry with respect to the sign of the bias voltage. Due to the positive sign of $e$, the homeotropic state is favoured by the positive voltage. The homeotropic state is stable in thicker layers when subjected to $U>0$ than when subjected to $U<0$. If the flexoelectric properties are weak (or if the flexoelectric nematic has large dielectric anisotropy), i.e. if

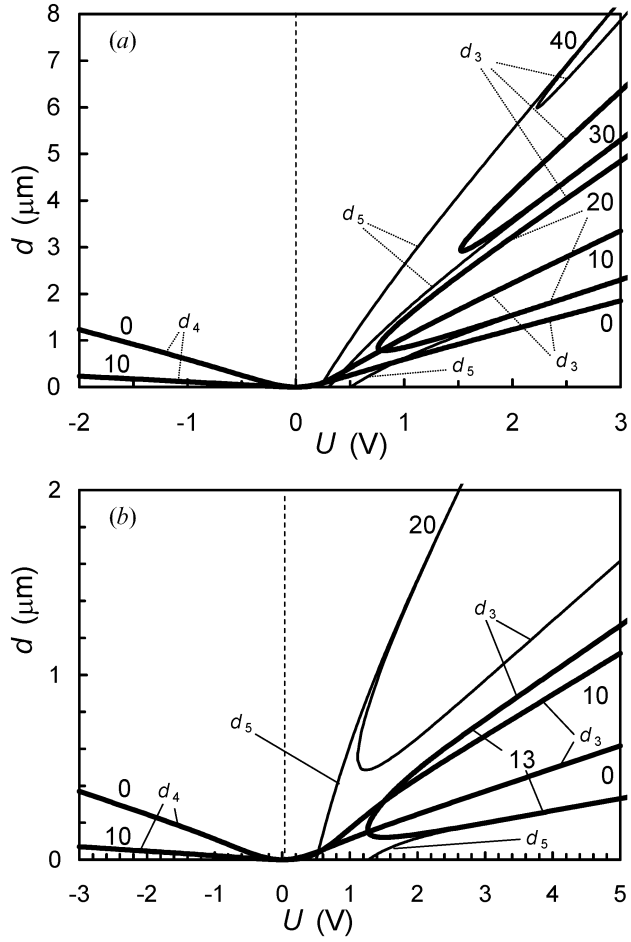


Figure 3. Regions of stability of the homeotropic state for $\Delta\varepsilon=2$ and $W_2=10^{-5}\,\mathrm{J\,m^{-2}}$. (a) $W_1=2\times10^{-5}\,\mathrm{J\,m^{-2}}$, (b) $W_1=10^{-4}\,\mathrm{J\,m^{-2}}$. The values of $e$ (in $\mathrm{pC\,m^{-1}}$) are indicated for each curve. The curves denoted by $d_3$ and $d_4$ result from condition (22), which is satisfied below them (for $e=0$ and $e=10\,\mathrm{pC\,m^{-1}}$) and in the regions surrounded by them (for $e=13$, 20, 30 and $40\,\mathrm{pC\,m^{-1}}$). The curves denoted by $d_5$ result from condition (23), which is satisfied in the areas above the curves. For $e=0$ and $e=10\,\mathrm{pC\,m^{-1}}$, the homeotropic state is stable in the areas below the thick curves. For other values of $e$, it is stable inside the regions limited by the thick curves.

$0<e_{11}+e_{33}\le\sqrt{k_{33}\varepsilon_0\Delta\varepsilon}$, the resulting ranges of $d$ are given by the product of equation (31) with equation (36) and by the product of equation (32) with equation (37). For the positive voltages one obtains $(0,\ vbL_1(g+1))$ and for the negative $(0,\ vbL_1(g-1))$. This means that the homeotropic state is stable in the regions of the $U,d$-plane included between the limit $d=0$ and the asymptotes $d=U\left(e_{11}+e_{33}+\sqrt{k_{33}\varepsilon_0\Delta\varepsilon}\right)/W_1$ [for $U>0$, equation (27)] and $d=U\left(e_{11}+e_{33}-\sqrt{k_{33}\varepsilon_0\Delta\varepsilon}\right)/W_1$ [for $U<0$, equation (29)]. In figures 3 a and 3 b, this case is presented for $e=10\,\mathrm{pC\,m^{-1}}$. If $g=1$, the homeotropic structure may appear only above the positive critical voltage.

(3) For moderate flexoelectric properties, $1<g\le(L_2+L_1)/(L_2-L_1)$, i.e. if $\sqrt{k_{33}\varepsilon_0\Delta\varepsilon}<e_{11}+e_{33}\le\sqrt{k_{33}\varepsilon_0\Delta\varepsilon}(W_1+W_2)/(W_1-W_2)$, the range of $d$ arises as a product of equations (33) and (36), which yields $(vbL_2(g-1),\ vbL_1(g+1))$. Therefore the region of stability of the homeotropic state in the $U,d$-plane is included between the asymptotes given by equation (27), $d=U\left(e_{11}+e_{33}+\sqrt{k_{33}\varepsilon_0\Delta\varepsilon}\right)/W_1$, and by equation (28), $d=U\left(e_{11}+e_{33}-\sqrt{k_{33}\varepsilon_0\Delta\varepsilon}\right)/W_2$. It narrows with increasing $e_{11}+e_{33}$ and disappears when $g=(L_2+L_1)/(L_2-L_1)$. This case is represented by $e=20\,\mathrm{pC\,m^{-1}}$ and $30\,\mathrm{pC\,m^{-1}}$ in figure 3 a and by $e=13\,\mathrm{pC\,m^{-1}}$ in figure 3 b. The homeotropic state is stable in the region limited by the branches of thick curves denoted by $d_3$. The layer thickness must exceed a certain minimum which is very low when $g$ is close to 1.

(4) For strong flexoelectric properties, $g>(L_2+L_1)/(L_2-L_1)$, (or if the parameter $g$ is enhanced due to small magnitude of dielectric anisotropy) i.e. if $e_{11}+e_{33}>\sqrt{k_{33}\varepsilon_0\Delta\varepsilon}(W_1+W_2)/(W_1-W_2)$, the range of $d$ results from the product of equations (34) and (36), which is an empty set. It means that the inequalities (22)–(23) are contradictory. The same applies to conditions (22)–(23). The homeotropic state is therefore unstable. This case is exemplified by $e=40\,\mathrm{pC\,m^{-1}}$ in figure 3 a and by $e=20\,\mathrm{pC\,m^{-1}}$ in figure 3 b. The inequality, which is given above to limit the sum $e_{11}+e_{33}$, can be rewritten in the form

$$\Delta\varepsilon<\left[(e_{11}+e_{33})^2\Big/k_{33}\varepsilon_0\right][(W_1-W_2)/(W_1+W_2)]^2. \tag{38}$$

The right hand side of equation (38) reveals the critical value of $\Delta\varepsilon$ below which the homeotropic state becomes unstable. This implies that the homeotropic state does not appear if $\Delta\varepsilon\leqslant 0$. This conclusion is essential for the cases considered in the next sections.

## 4. Negative dielectric anisotropy

In the case of a negative dielectric anisotropy, the dielectric torque favours the planar structure. The homeotropic state does not appear, which is implied from equation (38).

When $\Delta\varepsilon<0$, the bulk torque equation takes the form

$$\frac{\mathrm{d}^2\theta}{\mathrm{d}z^2}-\kappa^2\theta=0, \tag{39}$$

where $\kappa=(U/d)(\varepsilon_0|\Delta\varepsilon|/k_{11})^{1/2}$ and the sign "–" is due to the negative sign of the dielectric anisotropy. Its solution is given by $\theta(z)=M\cosh(\kappa z)+N\sinh(\kappa z)$, where $M$ and $N$ are constants. The truncated total free energy per unit area of the layer is given by

$$\begin{aligned}G=&\frac{1}{2}M^2k_{11}\left(\kappa sc+f\kappa s^2+1/L_1-c^2/L_2\right)\\&+MNk_{11}\left(\kappa s^2+f\kappa sc-sc/L_2\right)\\&+\frac{1}{2}N^2k_{11}\left(\kappa sc+f\kappa s^2-s^2/L_2\right),\end{aligned} \tag{40}$$

where $s=\sinh\kappa d=\sinh u$, $c=\cosh\kappa d=\cosh u$, $f=e(k_{11}\varepsilon_0|\Delta\varepsilon|)^{-1/2}$ and $u=U(\varepsilon_0|\Delta\varepsilon|/k_{11})^{1/2}$. The stability conditions lead to two inequalities:

$$\begin{aligned}-d^2+\mathrm{d}u[f(L_2+L_1)+(L_2-L_1)\coth u]\\+u^2\left(1-f^2\right)L_1L_2>0,\end{aligned} \tag{41}$$

$$-d+uL_2(\coth u+f)>0. \tag{42}$$

The solution of the quadratic inequality (41) is given by the formulae analogous to equations (24)–(26), i.e. $\min\left(d_6^+,d_6^-\right)<d<\max\left(d_6^+,d_6^-\right)$, for $U>0$, and $\min\left(d_7^+,d_7^-\right)<d<\max\left(d_7^+,d_7^-\right)$, for $U<0$. In the limit $u\to+\infty$, when $\coth u=1$, the critical thicknesses $d_6^{\pm}$ are

$$d_{6\infty}^-=uL_2(f+1) \tag{43}$$

and

$$d_{6\infty}^+=uL_1(f-1). \tag{44}$$

In the limit $u\to-\infty$, when $\coth u=-1$, the critical thicknesses $d_7^{\pm}$ are

$$d_{7\infty}^+=uL_1(f+1) \tag{45}$$

and

$$d_{7\infty}^-=uL_2(f-1). \tag{46}$$

These formulae give the equations of oblique asymptotes $d(U)$.

The inequality (42) is satisfied if $d<L_2u(\coth u+f)\equiv d_8$. For $U\to\infty$, the critical thickness $d_8$ tends to the asymptote $d=uL_2(f+1)$, identical to equation (43). For $U\to-\infty$, the asymptote is $d=uL_2(f-1)$ which coincides with equation (46).

As described in section 3.1, the parts of asymptotes corresponding to positive $d$ help to determine the superposition of equations (41)–(42). The resulting condition of stability of the planar state is identical with the inequality (41). For $0\leqslant f\leqslant 1$, the region of existence in the $U,d$-plane lies between $d=d_6^-$ and $d=0$ when $U>0$ and between $d=d_7^-$ and $d=0$ when $U<0$. If $f>1$, the inequality (41) gives two branches of the curve which limit the region of existence of the planar structure in the $U,d$-plane.

Figure 4 a shows several representative results for the finite planar anchoring strength. In figure 4 b, the case of a rigid planar anchoring is illustrated. Various sums of the flexoelectric coefficients are taken into account. In the non-flexoelectric nematic, the planar state is realized for any voltage. The critical thickness increases with $|U|$. The weak flexoelectricity ($f<1$) enhances the region of existence of the planar state induced by the positive voltage and diminished the region corresponding to the negative voltage (figure 4 a, $e=10\,\mathrm{pC\,m^{-1}}$). If the flexoelectric properties are sufficiently strong ($f>1$), the planar state appears in some range of thickness corresponding to given value of $U$ (figure 4 a, $e=20$, 30, $40\,\mathrm{pC\,m^{-1}}$).

If the planar anchoring is rigid, $L_1=0$, the planar state may exist if the layer is thinner than some critical value which depends on $U$ (figure 4 b).

If the anchoring strengths on the planar and homeotropic walls are identical, $L_1=L_2\equiv L$ then the planar state does not exist in the absence of the field. However, applied voltage of any magnitude induces the planar structure for the ranges of thickness bounded by the asymptote $d=uL(f+1)$ and $d=0$ if $0\leqslant f\leqslant 1$ and by two asymptotes $d=uL(f-1)$ and $d=uL(f+1)$ if $f>1$.

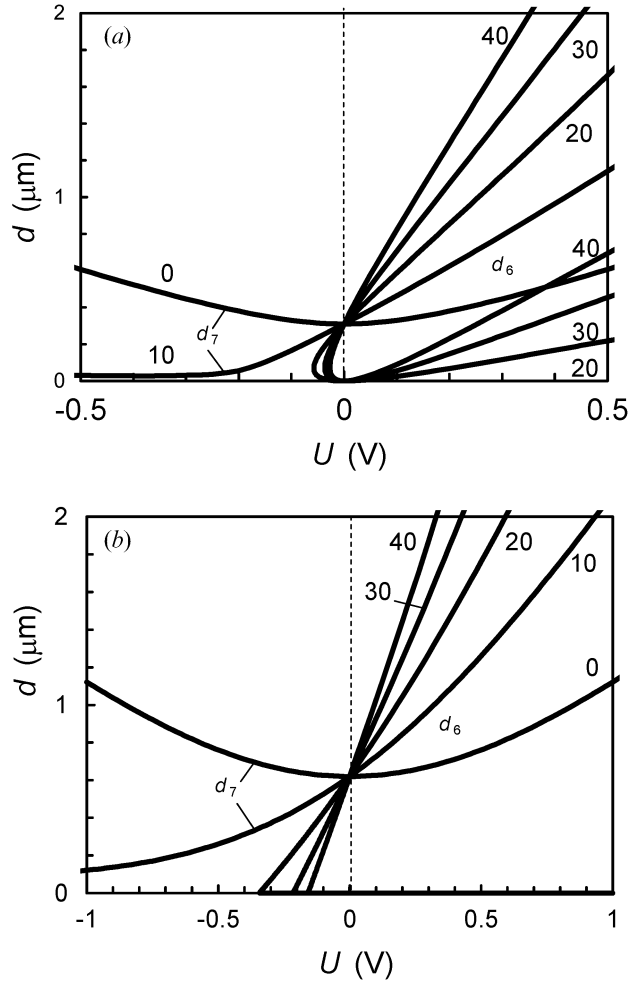


Figure 4. Regions of stability of the planar state for $\Delta\varepsilon=-2$ and $W_2=10^{-5}\,\mathrm{J\,m^{-2}}$. (a) $W_1=2\times10^{-5}\,\mathrm{J\,m^{-2}}$, (b) $W_1=\infty$. The values of $e$ (in $\mathrm{pC\,m^{-1}}$) are indicated for each curve. The curves result from the condition (41). The planar state exists below the curves (for $e=0$ and $e=10\,\mathrm{pC\,m^{-1}}$) and between the branches of them (for $e=20$, 30 and $40\,\mathrm{pC\,m^{-1}}$).

## 5. Dielectrically compensated nematic

In the case of $\Delta\varepsilon=0$, an external electric field exerts only flexoelectric torques. The homeotropic state does not appear, according to equation (38). Structural transitions occur only between the planar and distorted states.

When $\Delta\varepsilon=0$, the bulk torque equation takes the simple form $\mathrm{d}^2\theta/\mathrm{d}z^2=0$. Its solution is $\theta(z)=Pz+Q$, where $P$ and $Q$ are constants. The truncated total free energy per unit area of the layer is given by

$$G=P^2\left(k_{11}d+eUd-W_2d^2\right)/2 + PQ(eU-W_2d)+Q^2(W_1-W_2)/2. \quad (47)$$

The condition $\partial^2G/\partial Q^2>0$ is always satisfied in this case. Therefore the stability condition takes the form of the inequality

$$-d^2W_1W_2+d[(k_{11}+eU)(W_1-W_2)+2eUW_2] -e^2U^2>0. \quad (48)$$

The solution of this inequality is given in the form of equation (16).

$$d_9^+<d<d_9^-, \quad (49)$$

where $d_9^+$ and $d_9^-$ are given by formulae analogous to equation (17). In the limit $U\to\infty$, the range of thicknesses which satisfy the inequality (49) is determined by the asymptotes $d=eU/W_2$ and $d=eU/W_1$.

Figures 5 a and 5 b show several examples obtained for finite and infinite planar anchoring strength, respectively, and for various sums of the flexoelectric coefficients. In the case of a non-flexoelectric nematic, the planar state appearing for $d<L_2-L_1$ is unaffected by the voltage. If the nematic possesses the flexoelectric properties, the planar state may exist in a certain range of thickness at positive voltages and at negative voltages of sufficiently small magnitude (figure 5 a). If the anchoring strengths on the planar and homeotropic walls are identical, $W_1=W_2$, then $d_9^+=d_9^-$, which means that the planar state does not occur at any voltage. If the planar anchoring is rigid, $W_1=\infty$, the planar state exists for thickness smaller than a critical value $d_9^+=L_2+eU/W_2$ (figure 5 b).

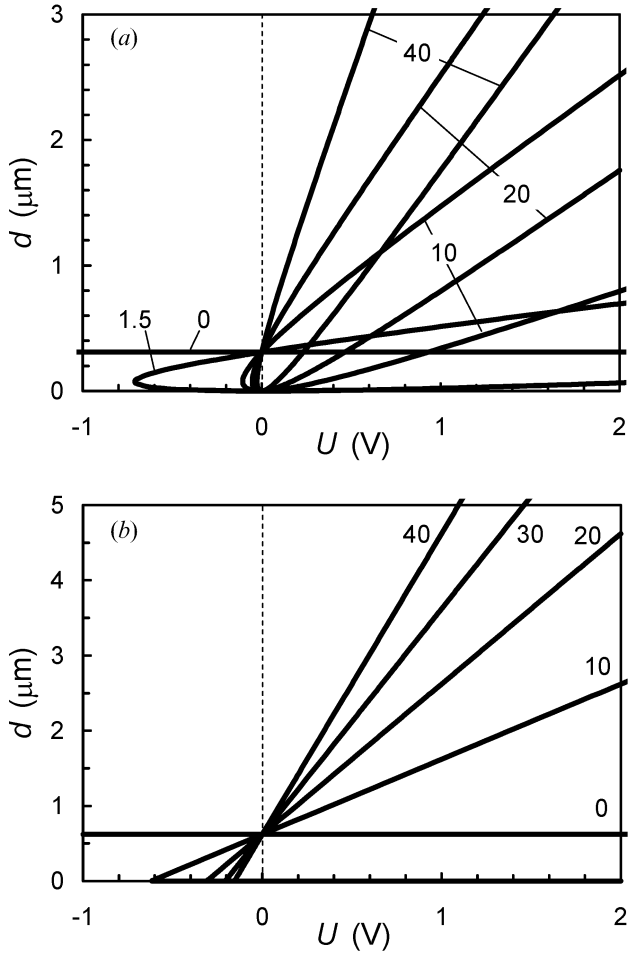


Figure 5. Regions of stability of the planar state for $\Delta\varepsilon=0$ and $W_2=10^{-5}\,\mathrm{J\,m^{-2}}$. (a) $W_1=2\times10^{-5}\,\mathrm{J\,m^{-2}}$, (b) $W_1=\infty$. The values of $e$ (in $\mathrm{pC\,m^{-1}}$) are indicated for each curve. The curves result from the condition (48). The planar state exists below the line corresponding to $e=0$ and between the branches of the curves (for $e>0$).

## 6. Examples of field-induced transitions in HAFN layers

In the following, the behaviour of the HAFN layers subjected to an electric field is illustrated by the results of numerical simulations. An insulating nematic material with elastic constants $k_{11}=6.2\,\mathrm{pN}$ and $k_{33}=8.6\,\mathrm{pN}$ was considered. The anchoring strength was $W_1=2\times10^{-5}\,\mathrm{J\,m^{-2}}$ on the planar surface and $W_2=10^{-5}\,\mathrm{J\,m^{-2}}$ on the homeotropic surface. The optical phase difference, $\Delta\Phi$, was used to characterize the state of the layer. The homeotropic structure was represented by $\Delta\Phi=0$, the planar state by $\Delta\Phi=2\pi d(n_e-n_o)/\lambda$, whereas the distorted structure is represented by an intermediate value, $\Delta\Phi=(2\pi/\lambda)\left(n_e d-\int_0^d \left[n_e n_o\Big/\left(n_e^2\cos^2\theta+n_o^2\sin^2\theta\right)^{1/2}\right]\mathrm{d}z\right)$, where $n_e=1.672$ and $n_o=1.520$ are the extraordinary and ordinary refractive indices, respectively, and the wavelength is $\lambda=632.8\,\mathrm{nm}$.

In the case of a positive dielectric anisotropy, there are several possible sequences of states realized when the positive voltage is increased from zero: distorted–homeotropic, planar–distorted–homeotropic, distorted–planar–distorted, distorted–planar–distorted–homeotropic–distorted and distorted–homeotropic–distorted. In the case of a negative dielectric anisotropy, the analogous transitions are planar–distorted, distorted–planar–distorted and distorted–planar. For sufficiently thin layers and small $f$, the planar state may exist for any $U>0$. Figure 6 shows three examples for $\Delta\varepsilon=2$ and two examples for $\Delta\varepsilon=-2$. The voltage ranges of the planar and homeotropic states agree with the theoretical predictions made in sections 3.1 and 3.2.

The horizontal sections of the plots positioned at $\Delta\Phi=0$ correspond to the homeotropic state and those for which $\Delta\Phi>0$ are due to the planar state. Curves 1–3 of figure 6 represent a nematic possessing positive dielectric anisotropy. Curve 1 shows the transition between the planar and homeotropic states with intermediate distorted hybrid states, possible in rather thin layers. These states belong to the stability regions depicted in figures 1 a and 3 a. Curve 2 corresponds to the case of weak flexoelectric properties for which the homeotropic state becomes stable above some critical voltage due to prevailing dielectric interaction. If the flexoelectric effect has moderate magnitude (curve 3) the stability of the homeotropic state is limited to a narrow voltage range. Both types of behaviour can be deduced from figure 3 a. Curves 4 and 5 exemplify the behaviour of a nematic with negative dielectric

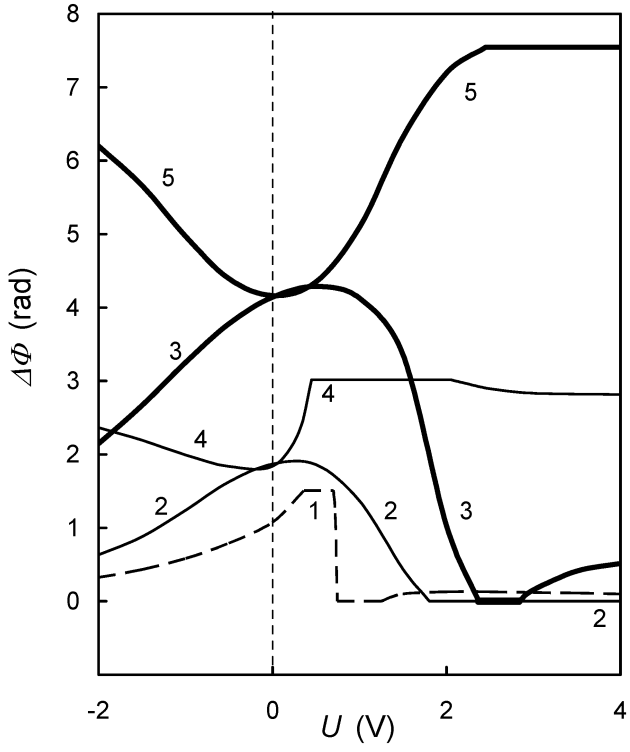


Figure 6. Phase retardation in the HAFN layer as a function of applied voltage; $W_1=2\times10^{-5}\,\mathrm{J\,m^{-2}}$, $W_2=10^{-5}\,\mathrm{J\,m^{-2}}$; curve 1: $\Delta\varepsilon=2$, $e=20\,\mathrm{pC\,m^{-1}}$, $d=1\,\mu\mathrm{m}$; curve 2: $\Delta\varepsilon=2$, $e=10\,\mathrm{pC\,m^{-1}}$, $d=2\,\mu\mathrm{m}$; curve 3: $\Delta\varepsilon=2$, $e=30\,\mathrm{pC\,m^{-1}}$, $d=5\,\mu\mathrm{m}$, curve 4: $\Delta\varepsilon=-2$, $e=30\,\mathrm{pC\,m^{-1}}$, $d=2\,\mu\mathrm{m}$; curve 5: $\Delta\varepsilon=-2$, $e=20\,\mathrm{pC\,m^{-1}}$, $d=5\,\mu\mathrm{m}$.

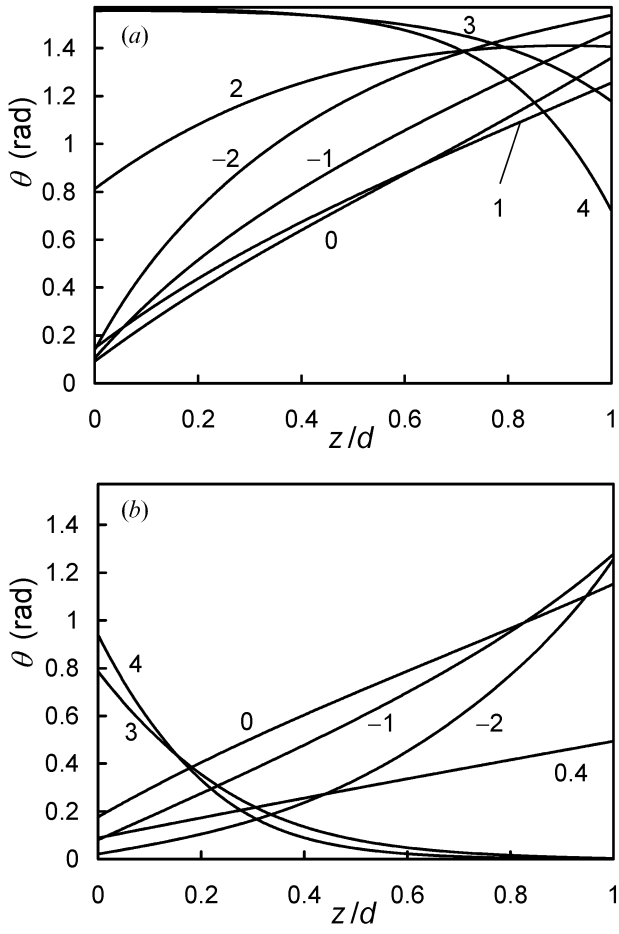


Figure 7. Director distributions in the distorted state of the HAFN layer: $W_1=2\times10^{-5}\,\mathrm{J\,m^{-2}}$, $W_2=10^{-5}\,\mathrm{J\,m^{-2}}$, $e=30\,\mathrm{pC\,m^{-1}}$; (a) $\Delta\varepsilon=2$, $d=5\,\mu\mathrm{m}$; (b) $\Delta\varepsilon=-2$, $d=2\,\mu\mathrm{m}$. The bias voltages (in volts) are indicated for each curve.

anisotropy, for which the homeotropic state does not appear. In both cases, the planar state exists in some voltage range which may be narrow (curve 4) or spread towards large $U$ (curve 5), as can be predicted from figure 4 a.

In figures 7 a and 7 b, typical director distributions in the distorted state are depicted by means of $\theta(z/d)$ plots for $\Delta\varepsilon=2$ and $\Delta\varepsilon=-2$, respectively. The director orientation in the bulk is influenced mainly by the dielectric torque. The orientations at the boundaries are a consequence of the flexoelectric, elastic and anchoring surface torques, which are included in equations (5)–(6).

The unaffected hybrid structure is represented in figures 7 a and 7 b by the nearly linear director profiles, $\theta(z/d)$, obtained for $U=0$. If $U<0$, the senses of the surface flexoelectric torques and anchoring torques coincide. As a result, the director at the boundaries approaches the easy axes directions, i.e. $\theta(0)\to0$ and $\theta(d)\to\pi/2$. The resulting structures are illustrated by the profiles plotted for $U=-1\,\mathrm{V}$ and $U=-2\,\mathrm{V}$. Differences in the shapes of the profiles for $\Delta\varepsilon>0$ (figure 7 a) and for $\Delta\varepsilon<0$ (figure 7 b) are caused by the bulk dielectric torques. When $U>0$, the surface flexoelectric torques and anchoring torques are opposite. In consequence the director deviates from the easy axes. Figure 7 a shows how this effect increases with the applied voltage (curves for $U=1$, 2, 3 and 4 V). For $U=1$ and 2 V, i.e. below the range of existence of the homeotropic state, the director distributions approach the homeotropic state and are qualitatively different from the structures occurring for $U=3$ and 4 V, i.e. above this range. The director distributions are affected by the bulk dielectric torque which in the vicinity of $z=0$ co-operates with the flexoelectric torque and maintains $\theta\approx\pi/2$ due to $\Delta\varepsilon>0$. A similar effect is illustrated in figure 7 b for $\Delta\varepsilon<0$. The director orientation tends to the planar state as shown by the curve for 0.4 V. The curves for $U=3$ and 4 V show the director distribution occurring above the range of existence of the planar state. The dielectric torque enhances the action of the flexoelectric torque and maintains the orientation $\theta\approx0$ in the neighbourhood of $z=d$.

## 7. Discussion

In summary, flexoelectric properties influence significantly the existence of planar, homeotropic and distorted states in a layer with hybrid surface alignment. In particular, the homeotropic state is unstable if flexoelectricity is sufficiently strong. The planar state is favoured by the flexoelectric properties. If $\Delta\varepsilon>0$, it may be induced in much thicker layers than in the case of a non-flexoelectric nematic. If $\Delta\varepsilon<0$, the voltage range, in which the planar structure exists, is shifted towards the lower values.

In this paper, the anchoring strength on the planar surface is assumed to be larger than that on the homeotropic surface. The opposite relationship, i.e. $W_1<W_2$, would give analogous properties of the HAFN layer. The homeotropic structure would be stable in the absence of the field and the planar structure would be induced by sufficiently large voltage if $\Delta\varepsilon<0$. Another assumption made in this paper is the positive sum of the flexoelectric coefficients. The negative sum would give the same results but for opposite signs of voltages, which is easily seen from equations (4)–(7).

The results presented in this paper are quantitatively valid only for sufficiently pure nematics in which the influence of the ionic space charge may be neglected. Additional calculations were carried out in order to find out how large ion content is acceptable, i.e. what values of ion concentration, $N$, do not change the boundaries, $d(U)$, of the regions of stability of the homeotropic or planar structures. The model of electrical properties of a nematic sample described in previous papers [15, 16] was used for this purpose. It was based on the weak electrolyte model, taking into account dissociation and recombination of ions. The mobilities of anions as well as their diffusion coefficients were assumed to be greater than those of cations. Two kinds of electrode contacts were considered: well conducting and strongly blocking. The ion concentration was of order $5\times10^{18}\,\mathrm{m}^{-3}$. (The effects induced by ions adsorbed on the electrodes, described by Barbero *et al.* [17, 18], were ignored, since the low ion content prevents the arising of enough significant surface charge density.) The results show that the discrepancy between perfectly insulating nematics and weakly conducting nematics is negligible. The data for $e=30\,\mathrm{pC\,m}^{-1}$ presented in figures 3 a and 1 a can serve as an example. For $d=5\,\mu\mathrm{m}$, the theoretical voltages limiting the homeotropic state are 2.36 and 2.83 V. The simulated values are almost identical: 2.36 and 2.84 V for the conducting electrodes and 2.36 and 2.81 V for the strongly blocking contacts. The differences are slightly larger for $d=8\,\mu\mathrm{m}$. For the conducting electrodes, the calculated voltages are 3.73 and 4.58 V instead of the theoretical values 3.78 and 4.53 V. In the case of blocking contacts the differences have similar magnitude, as the voltages are 3.75 and 4.50 V. For $d=2\,\mu\mathrm{m}$, the planar structure of the insulating layer is stable between 0.61 and 0.93 V. In the case of a conducting material, only the lower limit is slightly changed and equals 0.62 V for both types of electrode. The above values confirm that experiments carried out with a highly purified nematic (characterized by the specific resistance $10^{10}$–$10^{11}\,\Omega\,\mathrm{m}$) can be successfully interpreted by the theory elaborated for the perfectly insulating material. The discrepancies become unacceptable if $N$ exceeds $10^{19}\,\mathrm{m}^{-3}$ since they reach 0.1 V for $5\times10^{19}\,\mathrm{m}^{-3}$. Nevertheless, qualitative agreement between the results for conducting and insulating nematics is revealed by simulations performed for even higher ion concentrations, $N\sim10^{20}\,\mathrm{m}^{-3}$.

On the basis of the results presented in this paper, one may propose a method of measurement of the sum $e=e_{11}+e_{33}$. According to the above discussion, sufficient purity of the nematic material is of great importance because the ionic space charge may significantly change the stability conditions. In principle, experimental determination of voltages limiting the ranges of stability of the homeotropic and planar states for several values of thickness would yield data sufficient to fitting the values of $e$, $W_1$ and $W_2$, provided the elastic constants and the dielectric anisotropy are known. A wedge-like sample could be useful. However, the fitting procedure may turn out to be difficult or inaccurate. Therefore, some other approaches can be proposed in particular cases. They will be analysed below under the assumption that $e>0$.

In the case of a positive dielectric anisotropy, one may seek the planar structure. The rigid planar anchoring ($L_1=0$), ensuring the behaviour exemplified in figure 1 c, would be convenient. The maximum thickness at which the planar state is stable as well as the voltage $U_d$ corresponding to this thickness are related by the condition $\mathrm{d}\left(d_1^-\right)/\mathrm{d}u=0$, where $d_1^-$ is given by equation (17). Solution of the equation $\mathrm{d}\left(d_1^-\right)/\mathrm{d}u=0$ with respect to $u$ gives the formula for the flexoelectric parameter:

$$f=(u_d-\sin u_d\cos u_d)/\sin^2 u_d, \tag{50}$$

where $u_d=U_d(\varepsilon_0\Delta\varepsilon/k_{11})^{1/2}$. The value of $W_2$ is not necessary. This method is useful if the homeotropic anchoring is rather weak and if the dielectric anisotropy is small, since such parameters ensure the conveniently large maximum thickness.

The homeotropic structure exists only if $W_1$ is finite. Its ranges of stability depend on all the three parameters $e$, $W_1$ and $W_2$. Therefore, in order to find $e$, one has to determine also $W_1$ and $W_2$. Both polarities of the

external voltage should be used. The observation of the boundaries of the homeotropic region in the wedge-like sample can yield the slopes $dd/dv$ of the asymptotes (27)–(28) or asymptotes (27) and (29). The set of two equations can be built: $a_1=bL_1(g+1)$ and $a_2=bL_2(g-1)$ if both slopes are positive or $a_1=bL_1(g+1)$ and $a_2=bL_1(g-1)$ if one of the slopes is negative. In the former case, the third equation can be obtained. For this purpose, the minimum voltage $U_m$ at which the homeotropic state exists as well as the corresponding thickness $d_m$ should be determined. These values are due to the case $\Delta=0$ in equation (26) and therefore they are connected by the relation

$$d_m=\beta/2=v_m b[g(L_2+L_1)-(L_2-L_1)\coth v_m], \quad (51)$$

where $v_m=U_m(\varepsilon_0\Delta\varepsilon/k_{33})^{1/2}$. The flexoelectric parameter $g$ and the anchoring strengths $W_1$ and $W_2$ can be calculated from the set of the three equations. This approach is effective if $v_m$ is close to 1, since in the opposite case, equation (51) does not differ significantly from the combination of the previous two equations. If one of the slopes is negative, the quantities $d_m$ and $v_m$ do not exist and the third equation cannot be built. In such a case, the knowledge of $W_1$ or $W_2$ is necessary.

In the case of a negative dielectric anisotropy, the voltage ranges of existence of the planar structure are determined by the asymptotes given by equations (43)–(46). If the slopes of them can be determined experimentally, the flexoelectric parameter $f$ can be found, provided that the anchoring strengths $W_1$ and $W_2$ are known. Therefore the rigid planar anchoring seems to be convenient.

Flexoelectric properties play an important role in the principle of operation of ZBD displays [10, 11]. There are several possible geometries of ZBD display. In each geometry, switching between two stable director configurations occurs. In the earliest version, one configuration is practically homeotropic, the other is practically hybrid. All types of ZBD display rely on a micron-scale grating surface. Elastic deformations arising close to this non-planar substrate cause a flexoelectric polarization, which provides a crucial contribution to the switching torques induced by bias voltage pulses of suitable polarity. The grating surface imposes a kind of periodic boundary condition, which ensures bistable surface alignment [19]. A model approach describing this geometry adopts the effective boundary conditions, which can be expressed by a surface energy term exhibiting two distinct energy minima due to homeotropic and planar director orientations [11]. The complex periodic boundary conditions as well as their simplified model are essentially different from the boundary conditions existing in the HAFN layer considered in the present paper. Therefore, the results of this paper do not apply to the ZBD case.

Nevertheless, another application concerning display devices may be considered. As the flexoelectric effects are linear in electric field, flexoelectricity gives rise to asymmetry of the layer behaviour with respect to the zero voltage. Such asymmetry is evident from the $\Delta\Phi(U)$ dependence. The asymmetry is also manifested in the electro-optical characteristics of the considered systems. Such effects were observed experimentally [6, 7]. An electro-optical display based on the HAFN layer with $\Delta\varepsilon>0$ exhibiting the effects described in this paper would offer switching between the minimum transmission in the homeotropic state at positive voltage and the maximum transmission in the distorted state at properly chosen negative voltage. One may expect that such a switching process would be faster than in other types of displays, in which the switching to the bright state is induced only by the action of the anchoring torques. In the case of $\Delta\varepsilon<0$, the maximum transmission could be achieved in the planar state by suitable choice of the thickness, whereas the dark state would require properly chosen voltage to obtain suitable distorted structure.

## References


[1] S. Matsumoto, M. Kawamoto, K. Mizunoya. *J. appl. Phys.*, **47**, 3842 (1976).
[2] G. Barbero, R. Barberi. *J. Phys., Paris*, **44**, 609 (1983).
[3] G. Barbero, L.R. Evangelista. *An Elementary Course on the Continuum Theory for Nematic Liquid Crystals* Sec. 3.10., pp. 156–159, World Scientific, Singapore (2001).
[4] R.B. Meyer. *Phys. Rev. Lett.*, **22**, 918 (1969).
[5] A.G. Petrov. in *Physical Properties of Liquid Crystals: Nematics*, D.A. Dunmur, A. Fukuda, G.R. Luckhurst (Eds), p. 251, INSPEC, London (2001).
[6] N.V. Madhusudana, G. Durand. *J. Phys. Lett., Paris*, **46**, L-195 (1985).
[7] T. Takahashi, S. Hashidate, H. Nishijou, M. Usui, M. Kimura, T. Akahane. *Jap. J. appl. Phys., Pt. 1*, **37**, 1865 (1998).
[8] S. Ponti, P. Ziherl, C. Ferrero, S. Zumer. *Liq. Cryst.*, **26**, 1171 (1999).
[9] N.T. Kirkman, T. Stirner, W.E. Hagston. *Liq. Cryst.*, **30**, 1115 (2003).
[10] J.C. Jones, E.L. Wood, G.P. Bryan-Brown, V.C. Hui. *SID 98 Digest*, 859 (1998).
[11] A.J. Davidson, N.J. Mottram. *Phys. Rev. E*, **65**, 051710 (2002).
[12] S. Warrier, N.V. Madhusudana. *J. Phys., Paris II*, **7**, 1789 (1997).
[13] L.M. Blinov, M.I. Barnik, H. Ohoka, M. Ozaki, N.M. Shtykov, K. Yoshino. *Eur. Phys. J. E*, **4**, 183 (2001).
[14] A. Derzhanski, A.G. Petrov, M.D. Mitov. *J. Phys., Paris*, **39**, 273 (1978).
[15] G. Derfel, M. Buczkowska. *Liq. Cryst*, **32**, 1183 (2005).
[16] M. Buczkowska, G. Derfel. *Liq. Cryst*, **32**, 1285 (2005).

[17] G. Barbero, L.R. Evangelista, N.V. Madhusudana. *Eur. Phys. J. B*, **1**, 327 (1998).
[18] G. Barbero, L.R. Evangelista. *Liq. Cryst*, **30**, 633 (2003).
[19] C. Denniston, J.M. Yeomans. *Phys. Rev. Lett.*, **87**, 275505 (2001).

## Appendix

It can be shown that $d_2 > d_1^-$. Namely, the positive value $d_1^- = \beta/2 + \left(\beta^2 - 4\alpha\gamma\right)^{1/2}\Big/2$ is smaller than $\beta$ since $4\alpha\gamma$ is positive:

$$d_1^- < \beta. \qquad (A1)$$

The quantity $\beta$ can be written as $\beta = d_2 - uL_1(\cot u - f)$. Hence, $d_2 = \beta + uL_1(\cot u - f)$, which denotes that

$$d_2 > \beta, \qquad (A2)$$

since from equation (18) one obtains $\cot u > -f$ for positive $d_2$. Superposition of equations (A1)–(A2) gives $d_2 > d_1^-$.